Neurobiology of Disease

Functional Correction of CNS Phenotypes in a Lysosomal Storage Disease Model Using Adeno-Associated Virus Type 4 Vectors

Gumei Liu,[1] Inês Martins,[1] John A. Wemmie,[4] John A. Chiorini,[5] and Beverly L. Davidson[1,2,3]

Program in Gene Therapy, Departments of [1]Internal Medicine, [2]Neurology, [3]Physiology and Biophysics, and [4]Psychiatry, University of Iowa, Iowa City, Iowa 52242, and [5]The National Institutes of Health, Bethesda, Maryland 20892

Lysosomal storage diseases (LSDs) represent a significant portion of inborn metabolic disorders. More than 60% of LSDs have CNS involvement. LSD therapies for systemic diseases have been developed, but efficacy does not extend to the CNS. In this study, we tested whether adeno-associated virus type 4 (AAV4) vectors could mediate global functional and pathological improvements in a murine model of mucopolysaccharidosis type VII (MPS VII) caused by β-glucuronidase deficiency. Recombinant AAV4 vectors encoding β-glucuronidase were injected unilaterally into the lateral ventricle of MPS VII mice with established disease. Transduced ependyma expressed high levels of recombinant enzyme, with secreted enzyme penetrating cerebral and cerebellar structures, as well as the brainstem. Immunohistochemical studies revealed close association of recombinant enzyme and brain microvasculature, indicating that β-glucuronidase reached brain parenchyma via the perivascular spaces lining blood vessels. Aversive associative learning was tested by context fear conditioning. Compared with age-matched heterozygous controls, affected mice showed impaired conditioned fear response and context discrimination. This behavioral deficit was reversed 6 weeks after gene transfer in AAV4 β-glucuronidase-treated MPS VII mice. Our data show that ependymal cells can serve as a source of enzyme secretion into the surrounding brain parenchyma and CSF. Secreted enzymes subsequently spread via various routes to reach structures throughout the brain and mediated pathological and functional disease correction. Together, our proof-of-principal experiments suggest a unique and efficient manner for treating the global CNS deficits in LSD patients.

Key words: **lysosomal storage disease; mucopolysaccharidoses; β-glucuronidase; AAV4; CSF; perivascular; fear conditioning**

Introduction

Distinct lysosomal storage diseases (LSDs) are rare, but, as a group, they represent a significant proportion of severe inherited metabolic conditions. More than 60% of LSDs have CNS involvement, which remains a major challenge for patient therapies (Meikle et al., 1999). Among the LSDs with brain involvement is mucopolysaccharidosis type VII (MPS VII), an inherited disorder caused by the deficiency of β-glucuronidase, a lysosomal acid hydrolase involved in the stepwise degradation of glucuronic acid-containing glycosaminoglycans (Sly et al., 1973; Neufeld and Muenzer, 1995). In LSDs in general, and in MPS VII in particular, incompletely degraded substrates accumulate within lysosomes, interfere with cellular metabolism, and eventually impair the function of various organ systems. The progressive neurological dysfunction in MPS VII includes enlarged ventricles and mental retardation (Neufeld and Muenzer, 1995).

A mouse model of MPS VII with a single base pair deletion in mouse *gus*, encoding β-glucuronidase, was described previously (Birkenmeier et al., 1989). Homozygous mutant mice have no detectable enzyme activity and are phenotypically very similar to the human disease. Affected mice have a shortened life span, dwarfism, skeletal deformities including dysmorphic facial features, corneal clouding, and lysosomal storage material in multiple tissues (Vogler et al., 1990). Mutant mice appear normal at birth, and, at early ages, tissue sections from the CNS show limited lysosomal distention, no gross alteration of structures, and no detectable cell loss. However, by 3–4 weeks of age, lysosomal storage vacuoles become evident in the meninges, perivascular cells, neurons, and glia. Disease progresses with age to include extensive lysosomal pathology in the hippocampus, cerebral cortex, and thalamus (Levy et al., 1996; Heuer et al., 2002).

Therapies for some of the LSDs, including MPS VII, benefit from the biochemical properties of non-membrane-bound lysosomal enzymes. Many of these enzymes are secreted in addition to being directly targeted to the lysosome. Once secreted, they can be endocytosed by the same or neighboring cells via mannose-6-phosphate receptor mechanisms (for review, see von Figura and Hasilik, 1986; Kornfeld and Mellman, 1989). This process of cross-correction, coupled with as little as 1–3% of wild-type levels reversing storage, is beneficial; fewer cells need be genetically

Received May 16, 2005; revised Aug. 23, 2005; accepted Aug. 25, 2005.

This work was supported by National Institutes of Health Grant HD 33531. We thank Amy Poremba for help with behavioral studies, Xiaohua He for technical assistance, Jian Shao for help with EM and confocal analyses, Paul McCray and the Davidson laboratory for helpful discussions, and Christine McLennan for manuscript preparation.

Correspondence should be addressed to Dr. Beverly L. Davidson, 200 Eckstein Medical Research Building, University of Iowa, Iowa City, IA 52242. E-mail: beverly-davidson@uiowa.edu.

DOI:10.1523/JNEUROSCI.2936-05.2005

 0270-6474/05/259321-07$15.00/0

corrected, and recovery requires only a few percent of wild-type levels of enzyme activity. Nonetheless, therapies directed at correcting the CNS aspect of the disease are challenging.

To date, peripheral delivery of recombinant enzyme, corrected cells, or recombinant vectors to adult mice has not broadly corrected established deficits, in part because of the selective permeability of the blood–brain barrier (i.e., the inability of products within the vascular lumen to reach underlying brain parenchyma) (Bastedo et al., 1994; Sands et al., 1994; Stein et al., 2001). In contrast, direct intraparenchymal delivery of recombinant viruses or cells did improve CNS pathologies (Taylor and Wolfe, 1997; Ghodsi et al., 1999; Bosch et al., 2000; Frisella et al., 2001; Brooks et al., 2002; Meng et al., 2003). However, disease correction was often regionally restricted to the injected region or to cell bodies projecting to the injection site, although methods to enhance spread can improve the distribution of enzyme-positive cells (Xia et al., 2001). As a result, correction of established deficits via parenchymal delivery likely requires more than one injection (Brooks et al., 2002). However, scaling a multiple injection paradigm to human patients may be problematic, supporting the investigation of alternative approaches.

One mode for widespread distribution of enzyme within the CNS is via the CSF present in the ventricular, subarachnoid, and perivascular spaces (Virchow-Robin spaces). Because CSF can access the perivascular spaces lining vessels penetrating brain parenchyma, the introduction of enzyme into CSF should allow broad parenchymal distribution. The ependyma, a thin layer of highly differentiated multiciliated cells lining the ventricles, actively exchanges molecules with the CSF and is critical for CSF circulation (for review, see Del Bigio, 1995). As such, ependymal cells provide a cellular depot for secretion of enzymes into the CSF, including β-glucuronidase (Ghodsi et al., 1999). In this study, we used adeno-associated virus type 4 (AAV4), which transduces the ependyma with high efficiency (Davidson et al., 2000; Liu et al., 2005), to test whether constitutive secretion of β-glucuronidase into CSF could reverse existing lysosomal pathology and behavioral deficits in the MPS VII mouse model.

Materials and Methods

Experimental animals. MPS VII (B6.C-H-2^{bm1}/byBir-gus^{mps}/+) mice and heterozygous controls were obtained from The Jackson Laboratory (Bar Harbor, ME) and from our own breeding colonies. Animal maintenance conditions and experimental protocols were approved by the University of Iowa Animal Care and Use Committee.

Viral vectors. The AAV4 vector used in this study contains the RSV (the Rous sarcoma virus long-terminal repeat) promoter upstream from human β-glucuronidase cDNA sequences. The expression cassette was flanked by AAV2 inverted terminal repeats and packaged in AAV4 capsids by triple transfection with packaging and helper plasmids (Chiorini et al., 1997; Davidson et al., 2000). Viral titers, determined by quantitative PCR, were $1 - 10^{12}$ pt/ml.

Injections. Adult β-glucuronidase-deficient mice (6–8 weeks old) were anesthetized with ketamine (100–125 mg/kg) and xylene (10–12.5 mg/kg). AAV4 vectors (10 μl) were injected into the right lateral ventricle of the brain using a 30 gauge Hamilton syringe driven by a microinjector (Micro4; World Precision Instruments, Sarasota, FL) at 0.5 μl/min. The coordinates were 0.4 mm rostral to bregma, 1.0 mm lateral to midline, and 2.0 mm from pia surface.

Fluorometric enzyme activity assay. β-glucuronidase-deficient ($n = 4$ per group) and control mice ($n = 4$) were killed 4 weeks after injection. Hippocampi, cerebral cortices, cerebella, and brainstems were dissected and homogenized in lysis buffer: 20 mM Tris, pH 7.5, 140 mM NaCl, 10 mM β-mercaptoethanol, 0.25% saponin, and a protease inhibitor mixture. β-Glucuronidase activity was measured in homogenized tissues using 4-methylumbelliferyl-β-D-glucuronide (10 mM in 0.1 M acetate buffer, pH 4.8; Sigma, St. Louis, MO) as substrate. Stop buffer (320 mM glycine and 200 mM carbonate buffer, pH 10.0) was added to terminate the reaction after 1 h of incubation at 37°C. Fluorescence was measured at 390 nm excitation and 460 nm emission. Enzyme activity is expressed as units per milligram of protein. One unit represents the amount of enzyme activity that will hydrolyze 1.0 nmol of substrate per hour per milligram of protein.

In situ *enzyme activity assay.* Mice were perfused with 2% paraformaldehyde and 2% glutaraldehyde in PBS. Brains were harvested and embedded in OCT compound (Sakura, Tokyo, Japan). Sections (16 μm) were washed with 0.05 M NaOAc buffer, pH 4.5, for 10 min and then incubated at 37°C for 40 min in 0.25 mM naphthol-AS-BI-β-D-glucuronide (Sigma) in 0.05 M NaOAc buffer, pH 4.5. Sections were then stained for 2–4 h at 37°C with 0.25 mM naphthol-AS-BI-β-D-glucuronide in 0.05 M NaOAc buffer, pH 5.2, with 1:500 2% hexazotized pararosaniline. Removal of β-D-glucuronide by β-glucuronidase leaves a water-insoluble, red precipitate. Sections were counterstained with 0.5% methyl green solution.

Morphological assays. After perfusion, brains of MPS VII mice were fixed in 2.5% glutaraldehyde at 4°C overnight. Tissues were then blocked and postfixed in 1% OsO_4 for 2 h at room temperature. After washing, dehydration, and infiltration, samples were embedded in JB4 or Epon compound. Sections (1 μm) were stained with toluidine blue solution and analyzed for cell morphology using an Olympus (Tokyo, Japan) BX-51 digital light microscope. The hippocampus, the cerebral cortex, and the striatum were examined further for semiquantitative evaluation of lysosomal storage. Approximately 200 cells were examined per region per brain. Three groups of mice were analyzed: heterozygous controls ($n = 3$), untreated MPS VII mice ($n = 3$), and treated MPS VII mice ($n = 6$).

Immunohistochemistry. Immunohistochemistry (IHC) was done on OCT embedded tissues. Goat anti-β-glucuronidase (1:100; a gift from Dr. William Sly, St. Louis University, St. Louis, MO) and rat anti-platelet endothelial cell adhesion molecule (PCAM) CD31 (1:100; Molecular Probes, Eugene, OR), were diluted in PBS with 3% BSA, 0.3% Triton X-100, and 0.02% NaN_3. Sections were incubated with primary antibodies overnight at 4°C followed by 2 h at room temperature with secondary antibodies (donkey anti-goat and donkey anti-rat at 1:200; Molecular Probes). Microscopy was conducted with a Zeiss (Oberkochen, Germany) 510 confocal microscope. For substrate assays, frozen sections were incubated with primary antibodies against chondroitin sulfate or heparan sulfate (mouse biotin-conjugated anti-chondroitin-6-sulfate antibody, 1:100; and mouse anti-heparan sulfate, 1:100; Seikagaku Corporation, Tokyo, Japan) at 4°C overnight followed by DAB staining.

Context fear conditioning. The experiments were performed in a fear-conditioning chamber connected to a computerized fear-conditioning system (Med Association, San Diego, CA). The setting included a Plexiglas chamber with a removable shock grid floor made of stainless-steel rods. A programmable animal shocker for footshock delivery at different intervals and intensities was connected to the grid. A camcorder was placed in front of the test chamber, and all animal activities were videotaped. The chamber was cleaned with Windex (SC Johnson, Racine, WI) before individual animals were placed into the chamber. Heterozygous controls ($n = 8$), untreated MPS VII mice ($n = 8$), and treated MPS VII mice ($n = 9$) were subjected to context fear-conditioning tests. Briefly, after 3 min of acclimation to the chamber (context 1), mice received seven successive shocks (2 min apart; footshock, 0.75 mA, 50 Hz, 1 s). Fear response was measured by freezing, which was defined as no movement other than respiratory activity. Freezing in the first 3 min after placement into the chamber was recorded during the training and again 24 h later in two contexts. Context 1 was the one used for training. Context 2 was a modified chamber with new olfactory, tactile, and visual cues. Animals stayed in their home cages during the 2 h interval between testing in the two contexts.

Statistical analysis. Average freezing time during the first 3 min after animals were placed into the chamber was recorded and analyzed. Freezing was expressed as mean ± SEM seconds per minute. Data were analyzed by one-way ANOVA, followed by Fisher's PLSD *post hoc* analysis for comparison between groups (StatView software; SAS Institute, Cary, NC). Paired Student's *t* tests were used for comparisons within groups.

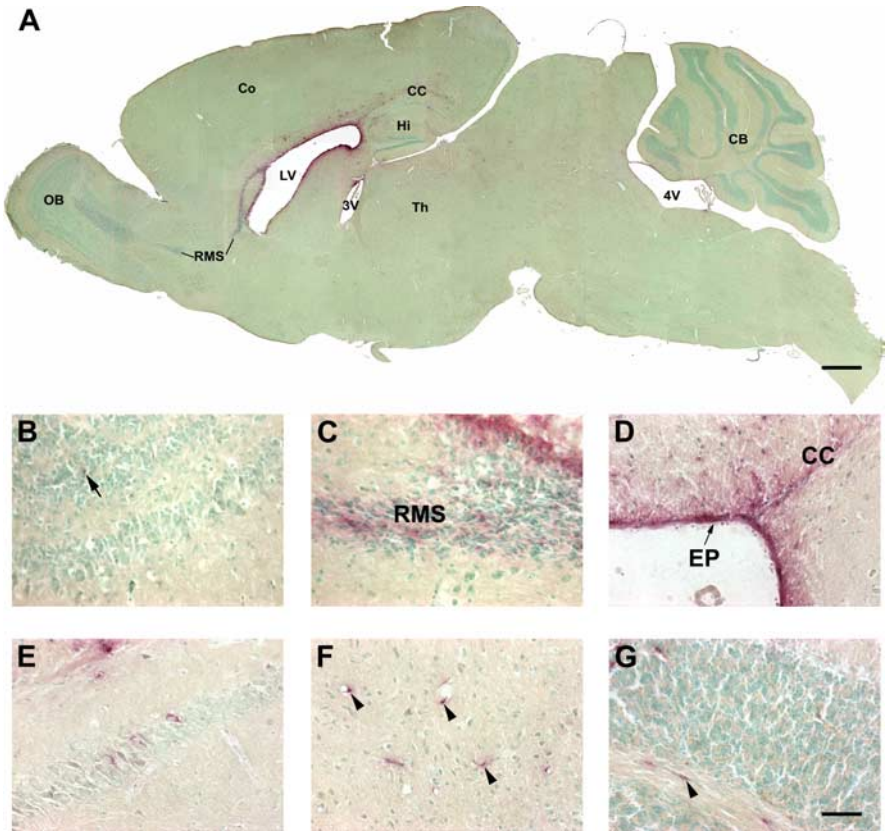

Figure 1. β-Glucuronidase distribution at 4 weeks after intraventricular injection. β-glucuronidase activity was revealed by *in situ* assay. Enzyme expression is observed throughout the brain, bilaterally, with highest staining density along the ventricular system. ***A***, Low-power photomicrograph showing β-glucuronidase activity throughout the brain of treated MPS VII mice. Scale bar, 400 μm. ***B–G***, Higher magnification of selected regions including the olfactory bulb (***B***; arrow, positive cell in granule cell layer), the RMS (***C***), the ependyma (EP) and corpus callosum (***D***), the CA3 region of the hippocampus (***E***), the thalamus (***F***), and the cerebellum (***G***). Some positive cells are associated with small vessels (arrowheads). Scale bar, 50 μm. LV, Lateral ventricle; 3V, the third ventricle; Hi, hippocampus; CC, corpus callosum; Th, thalamus; 4V, the fourth ventricle; CB, cerebellum, Co, cortex.

Results

AAV4 delivery to the lateral ventricle increases β-glucuronidase activity throughout the brain

A single dose of AAV4 encoding β-glucuronidase (AAV4βgluc) was injected into the lateral ventricle of adult MPS VII mouse brain. Treated mice were killed 4 weeks after injection for β-glucuronidase activity assays. Enzyme distribution was evaluated by *in situ* activity assay (Fig. 1). β-Glucuronidase activity was evident throughout the ventricular system (Fig. 1*A*) of both hemispheres. Consistent with direct transduction by AAV4, enzyme staining was most robust in the ependyma lining the ventricular system. Some distinct areas close to the lateral ventricle, for example, the fimbria and the CA3 region of the hippocampus, showed enhanced β-glucuronidase staining, likely attributable to local diffusion (Fig. 1*E*). The distribution of β-glucuronidase was graded in the parenchyma surrounding the ventricles, and, in general, the intensity of staining was inversely proportional to the distance from the ventricular lumen (Fig. 1*D*). The rostral migratory stream (RMS) was an exception to this, however, with more intense substrate deposition compared with surrounding areas (Fig. 1*A*,*C*). The intensity of β-glucuronidase staining decreased gradually along the caudal–rostral axis of the RMS (Fig. 1*A*). β-Glucuronidase$^+$ cells, albeit rare, were also found in the granule cell layer of the olfactory bulb (Fig. 1*B*, arrow).

Scattered β-glucuronidase$^+$ cells were noted in areas remote to the ventricles throughout the brain. Figure 1, *F* and *G*, shows representative staining in the thalamus and cerebellum. Most positive cells were associated with structures that morphologically resemble small blood vessels (Fig. 1*F*,*G*, arrows). IHC for β-glucuronidase and CD31 (a marker for endothelial cells; also known as PCAM) was done to determine whether enzyme-positive cells were brain vascular endothelia. As shown in Figure 2, anti-β-glucuronidase$^+$ cells were associated closely with CD31$^+$ endothelial cells in small vessels, but colocalization was not evident. The association of enzyme activity and vascular endothelia indicates that β-glucuronidase probably reaches the brain parenchyma via CSF in the perivascular spaces.

The *in situ* enzyme activity assay provides a qualitative measure of biodistribution after gene or enzyme transfer. To quantify levels of correction, fluorometric assays were done. We found no detectable β-glucuronidase activity in untreated MPS VII mice (data not shown). However, β-glucuronidase activity in AAV4βgluc-treated mice reached 34.80 ± 14.39, 27.69 ± 9.82, 11.79 ± 3.71, and 35.74 ± 1.89% (mean ± SEM) of heterozygous levels in hippocampi, cerebral cortices, cerebella, and brainstem, respectively (Fig. 3).

Biochemical and pathological changes after treatment

The major substrates accumulating in MPS VII are heparan and chondroitin sulfates (Neufeld and Muenzer, 1995). We used IHC to test whether substrate accumulation could be detected in affected mice, providing a separate and novel measure of efficacy. In MPS VII mice, both substrates were evident by IHC, with intracellular and extracellular spaces demonstrating immunoreactivity (Fig. 4*A*,*C*,*E*,*G*). Importantly, age-matched heterozygous littermates did not show substrate accumulation (supplemental figure, available at www.jneurosci.org as supplemental material). Intraventricular injection of AAV4βgluc to MPS VII mice dramatically reduced chondroitin sulfate and heparan sulfate immunoreactivity in all sections evaluated (Fig. 4*B*,*D*,*F*,*H*).

Progressive lysosomal storage and distension is a hallmark of the pathological changes in MPS VII patients and β-glucuronidase-deficient mice. At 6 weeks of age, the time of injection, lysosomal distension is evident throughout the CNS of MPS VII mice. By 10–12 weeks, the bubble-like lysosomal vacuoles are larger and more prevalent (Fig. 5). The ependyma, cerebral cortices, striata, and cerebella are affected to varying degrees (Fig. 5*A*,*E*,*I*,*K*), whereas the meninges and the CA3 region of the hippocampus showed extensive storage (Fig. 5*C*,*G*). In contrast, age-matched MPS VII mice treated with AAV4βgluc had limited storage. Lysosomal distention in the ependyma was completely cleared (Fig. 5*B*). Although some glial cells showed a minimal amount of storage, lysosomal distension was completely resolved in neurons in the hippocampus and striatum (Fig. 5*H*,*J*). Pathological improvement was also significant in the meninges and the cerebral cortices (Fig. 5*D*,*F*). AAV4βgluc treatment also reduced

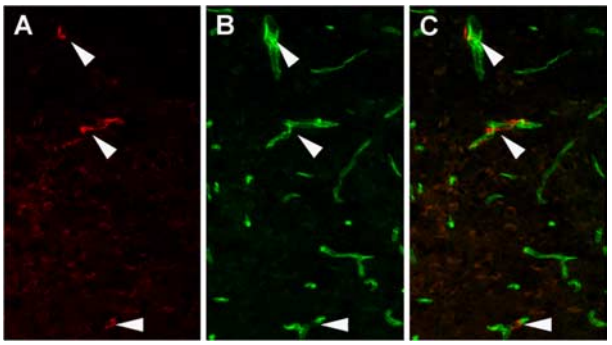

Figure 2. β-Glucuronidase-positive cells are in close association with the brain vasculature. ***A–C***, Immunohistochemistry for β-glucuronidase (***A***; red) and PCAM CD31 (***B***; green), an endothelial cell marker, reveals close association but not overlap (***C***; merge). Arrowheads denote β-glucuronidase-positive cells.

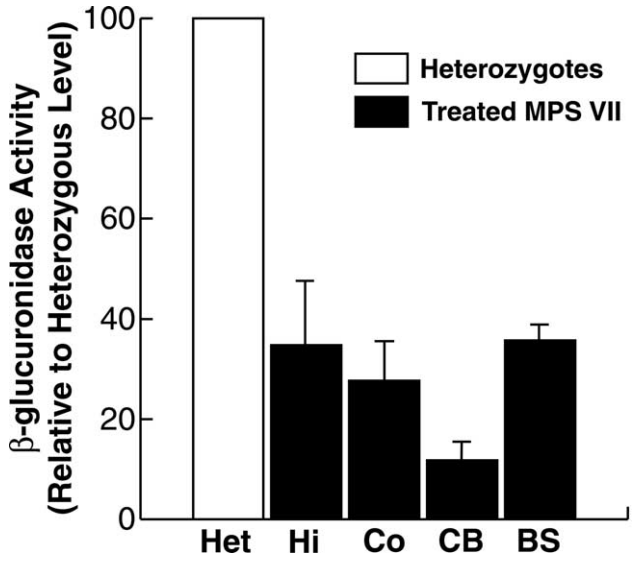

Figure 3. β-Glucuronidase activity levels in the brain. Data are shown as percentage of heterozygous levels and are mean ± SEM. Het, Heterozygotes; Hi, hippocampus; Co, cortex; CB, cerebellum; BS, brainstem. Error bars represent SEM.

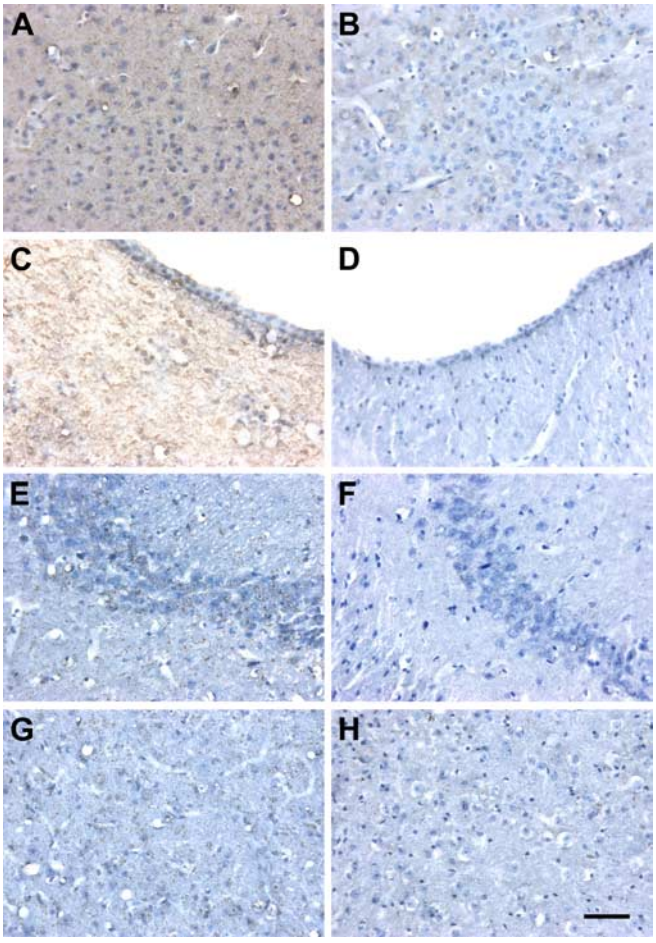

Figure 4. The effects of AAV4βgluc delivery on substrate levels in MPS VII mouse brain. ***A–H***, Substrate levels were assessed using anti-chondroitin sulfate (***A–D***) and anti-heparan sulfate (***E–H***) antibodies. ***A***, ***C***, ***E***, ***G***, In untreated MPS VII mice, substrate accumulation was notable in the extracellular spaces and cytoplasm. ***B***, ***D***, ***F***, ***H***, At 4 weeks after injection, chondroitin and heparan sulfate levels in AAV4βgluc-treated MPS VII mice decreased and were indistinguishable from sections harvested from normal littermates. Scale bar, 50 μm.

the size and number of lysosomal storage vacuoles in the mitral cells and granule cell layers of the olfactory bulb (Fig. 5*N*).

We next tested whether gene transfer to the cerebral lateral ventricle, and subsequent ependymal transduction, was sufficient for correction of the storage phenotype in the cerebellum. In storage disease therapies, cerebellar neurons were spared without directed delivery (Griffey et al., 2004). We found that a single injection of AAV4βgluc reduced storage in the Purkinje cells, granule cells, and cells in the molecular layer (Fig. 5*L*). Thus, existing cellular pathology and substrate accumulation in the cerebrum, cerebellum, and brainstem can be corrected within 4 weeks after AAV4βgluc-mediated gene transfer to the ependyma.

Semiquantitative analysis of lysosomal storage was performed in three brain regions: the CA3 region in the hippocampus, the motor cortex, and the striatum. Approximately 200 cells per region in each brain were examined for the presence of storage vacuoles. The results are shown as the percentage of cells that have visible lysosomal storage (mean ± SEM) (Fig. 6). In untreated MPS VII brains, the majority of cells had enlarged lysosomes, with 99.17 ± 0.83, 83.98 ± 2.66, and 54.67 ± 2.89% of cells positive for storage vacuoles in the hippocampus, the cerebral cortex, and the striatum, respectively. In contrast, heterozygous brains were virtually devoid of lysosomal storage. In AAV4βgluc-treated MPS VII mice, a dramatic reduction of storage-containing cells was observed in all three regions examined. The most evident improvement was seen in the hippocampus, in which only 1.51 ± 0.42% of total cells had storage vacuoles in treated MPS VII mice. Where present, vacuoles were of smaller size and number than those found in hippocampal cells from untreated MPS VII mice.

Intraventricular injection of AAV4βgluc improves existing behavioral deficits

The progressive impairment in the CNS of MPS VII mice causes measurable behavioral changes. Spatial learning tests, using the Morris water maze or the repeated acquisition and performance chamber (RAPC), show that β-glucuronidase-deficient mice have normal spatial learning at an early age but become progressively and measurably impaired by 6–8 weeks relative to heterozygous littermates (Chang et al., 1993; O'Connor et al., 1998; Brooks et al., 2002). The Morris water maze is not applicable to adult MPS VII mice because of their progressive systemic disease, and the successive water/food deprivation cycles required for the RAPC result in substantial testing-associated stress and death.

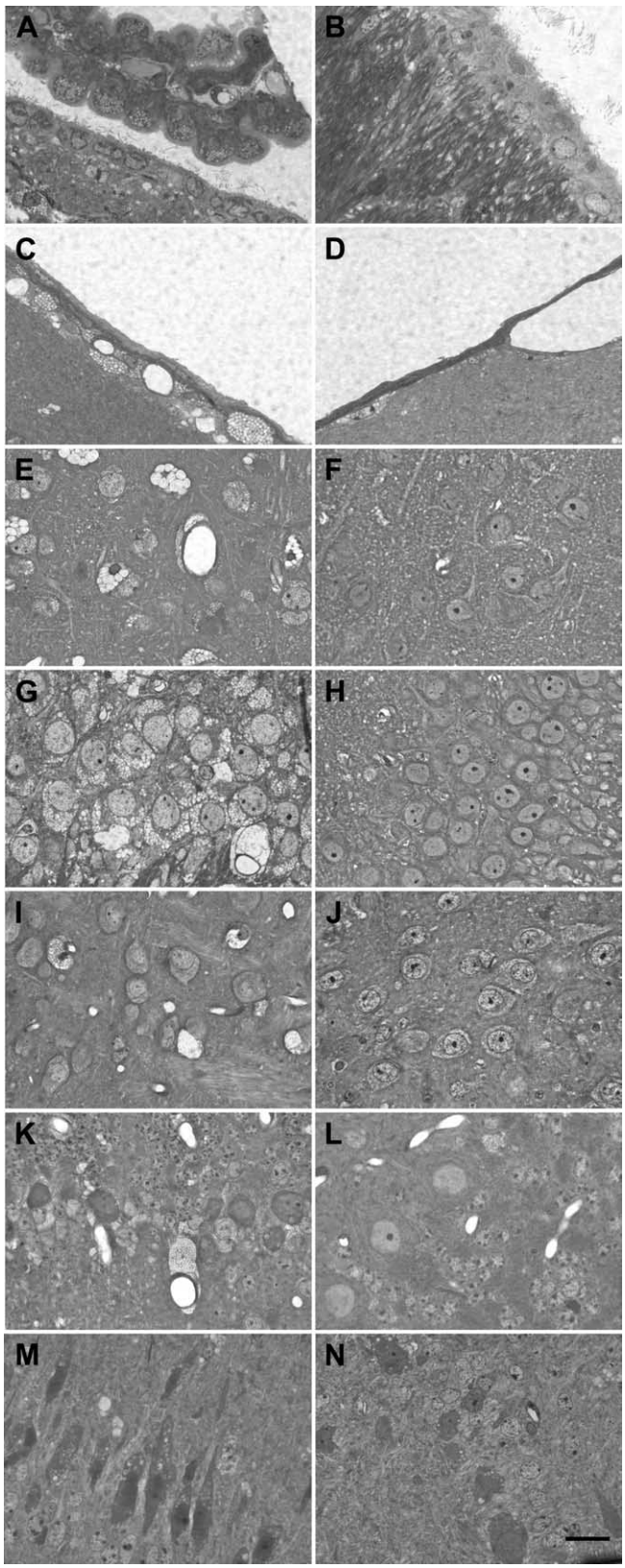

Figure 5. CNS pathology is improved after AAV4βgluc delivery to the lateral ventricles of MPS VII mice. ***A–M***, Lysosomal storage is observed throughout the brain in untreated (***A***, ***C***, ***E***, ***G***, ***I***, ***K***, ***M***) but reduced in treated (***B***, ***D***, ***F***, ***H***, ***J***, ***L***, ***N***) mutant mice. ***G–J***, The hippocampus (***G***, ***H***) and the striatum (***J***) are nearly devoid of remaining storage 4 weeks after gene transfer. ***A–N***, Evaluation of the ependyma (***A***, ***B***), meninges (***C***, ***D***), cerebral cortex (***E***, ***F***), cerebellum (***K***, ***L***), and olfactory bulb (***M***, ***N***) shows extensive improvements in lysosomal distention after AAV4βgluc delivery. Scale bar, 20 μm.

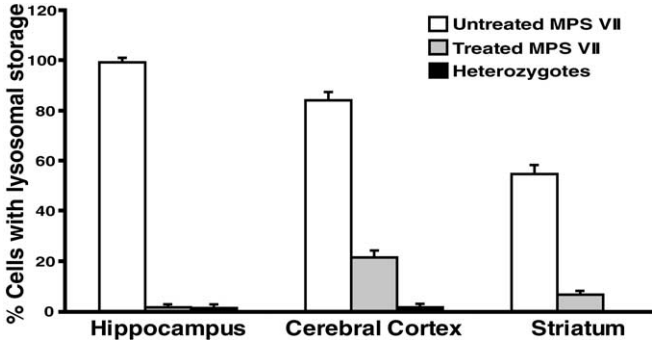

Figure 6. AAV4βgluc reduces lysosomal storage vacuoles in MPS VII mice brain. Cells in the hippocampus, cerebral cortex, and striatum were assessed for the presence or absence of storage vacuoles. Data are presented as percentage of cells ± SEM. Error bars represent SEM.

Therefore, we used context fear-conditioning assays to test the effects of AAV4βgluc therapy.

As shown in Figure 7*A*, heterozygous mice explored the context 1 chamber actively, with minimal freezing before training (average baseline freezing time, 0.52 ± 0.26 s/min). Before the shocks, treated and untreated MPS VII mice showed comparable baseline freezing time (12.50 ± 1.84 and 10.21 ± 1.81 s/min, respectively; $p = 0.31$; Fisher's PLSD), with both groups showing significantly higher baseline freezing than their normal control littermates ($p < 0.0001$; Fisher's PLSD). These results likely reflect the fact that MPS VII mice are less active than heterozygous controls because of established peripheral diseases.

Heterozygous, AAV4βgluc-treated MPS VII mice, and untreated MPS VII mice showed conditioned fear responses, measured as increased freezing time after placement back into context 1 the following day (Fig. 7*B*) (26.27 ± 1.70, 24.67 ± 2.02, and 13.63 ± 2.59 s/min, respectively). Of note, the increase in freezing time in AAV4βgluc-treated MPS VII mice significantly improved and was comparable with that measured for heterozygous mice (treated mutant mice vs heterozygotes; $p = 0.63$; Fisher's PLSD). In contrast, untreated MPS VII mice showed impaired conditioned fear responses relative to heterozygous mice and treated MPS VII mice ($p < 0.0001$ for both comparisons; Fisher's PLSD).

We next assessed context discrimination in treated and untreated MPS VII mice and their heterozygous littermates. As shown in Figure 7*C*, heterozygous controls froze less often in context 2 relative to context 1 (−15.96 ± 1.91 s/min; $p < 0.0001$; paired *t* test). The decrease in freezing time indicates that heterozygous mice can distinguish between the two contexts. Untreated MPS VII mice were unable to discriminate contexts, because they froze for similar durations in context 1 and context 2 (−1.92 ± 2.05 s/min; $p = 0.23$; paired *t* test). For AAV4βgluc-treated MPS VII mice, the fear response in context 2 was significantly reduced relative to context 1 (−17.70 ± 1.69 s/min; $p < 0.0001$; paired *t* test), paralleling the response seen in normal mice. Both heterozygous and AAV4βgluc-treated MPS VII mice groups show responses significantly different from untreated MPS VII mice ($p < 0.0001$; Fisher's PLSD). Thus, intraventricular injection of AAV4βgluc was sufficient to correct context discrimination deficiencies inherent in MPS VII mice.

Discussion

Our previous work showed that intraventricular injection of AAV4 expressing nonsecreted reporter genes transduced ependyma exclusively (Davidson et al., 2000; Liu et al., 2005). In

this study, we found evidence of enzyme activity beyond the transduced ependyma after intraventricular injection of AAV4βgluc, including corrected storage pathology in cerebrum and cerebellum and improvements in established behavioral deficits. These results are very encouraging and support the hypothesis that therapeutic success for the mucopolysaccharidoses, and for LSDs in general, benefits significantly from cross-correction, a process whereby affected cells take up soluble enzymes from the surrounding environment (Frantantoni et al., 1969; Neufeld and Fratantoni, 1970; Neufeld and Muenzer, 1995).

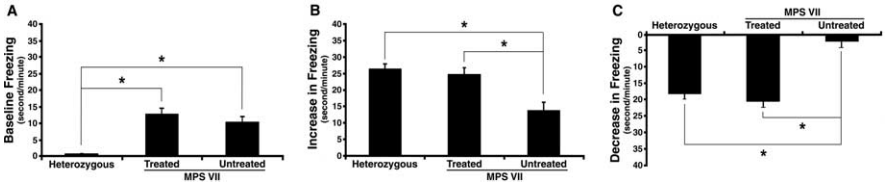

Figure 7. AAV4βgluc reverses behavioral deficits in MPS VII mice in context fear-conditioning assays. One-way ANOVA revealed group ($n = 3$, heterozygous, treated, and untreated MPS VII mice) as a significant factor ($F_{(2,220)} = 10.754$; $p < 0.0001$). ***A***, Baseline measurements in context 1, day 1. Both treated and untreated MPS VII mice have significant elevated baseline levels of freezing compared with heterozygous controls (*$p < 0.0001$; Fisher's PLSD). ***B***, The increase in freezing time from baseline after placement in context 1 on day 2. Results from treated MPS VII mice and heterozygotes are comparable ($p = 0.63$; Fisher's PLSD). Increases in freezing time for untreated MPS VII mice were significantly less than the other groups (*$p < 0.0001$; Fisher's PLSD). ***C***, Difference in freezing time between context 1 and 2, day 2. Compared with untreated MPS VII mice, treated MPS VII mice and heterozygous controls freeze significantly less in context 2 compared with context 1 (*$p < 0.0001$; Fisher's PLSD). Error bars represent SEM.

Routes of β-glucuronidase distribution

The secretion of β-glucuronidase from transduced ependyma into the CSF works in concert with cross-correction to extend the zone of therapeutic benefit. The distribution of β-glucuronidase in the CNS after secretion from transduced ependyma can occur by several routes. First, β-glucuronidase may reach adjacent areas by local diffusion (Fig. 1). We know from this work and from previous studies (Ghodsi et al., 1999; Xia et al., 2001) that the depth of diffusion, as assessed by *in situ* enzyme staining or the more sensitive evaluation of storage pathology, is limited. Modifications to β-glucuronidase, for example, the addition of a domain to reduce uptake by the mannose-6-phosphate receptor (Xia et al., 2001; Orii et al., 2005), can improve the parenchymal distribution of enzyme secreted from transduced cells.

Local diffusion may also be responsible in part for the intense enzyme activity in the RMS relative to nearby regions (Fig. 1). The RMS is enriched in neuroblasts en route from the subventricular zone (SVZ) to the olfactory bulb (OB). Neuroblasts ultimately differentiate into OB interneurons in the granule and periglomerular cell layers (for review, see Gage, 2000). Enzyme diffusing into the extracellular space of the subependymal region from the ventricular spaces would be endocytosed by resident neuroblasts in the SVZ and caudal RMS. As neuroblasts traverse the RMS, enzyme would be secreted along the tract. We noted a reduction in staining intensity from caudal to rostral direction, with scattered enzyme-positive cells in the granule cell layer of the olfactory bulb, consistent with this possibility. Work by Passini et al. (2002) also shows that β-glucuronidase in the extracellular spaces can be endocytosed by migrating neuroblasts residing in the RMS. A second possibility for the elevated β-glucuronidase activity in the RMS would be direct transduction of neuroblasts or progenitor cells in the SVZ. This is unlikely, however, because intraventricular injection of AAV4 exclusively transduces ependyma and not neuroblasts or SVZ progenitors (Liu et al., 2005).

Our results are most consistent with the white matter tracts and perivascular spaces being the preferential routes for interstitial fluid movement in the brain (Abbott, 2004). As an example of the former, we found that β-glucuronidase activity, as assessed by *in situ* enzyme stain, was relatively intense along the corpus callosum (Fig. 1). In support of the perivascular delivery route, we found enzyme-positive cells closely associated with the microvasculature throughout the brain (Fig. 2) and widespread correction of the CNS pathology (Figs. 4–6).

CSF flow is likely critical for perivascular distribution of β-glucuronidase to the brain. Recombinant β-glucuronidase secreted into the ventricular lumen would be carried by the CSF through the third and fourth ventricles into the subarachnoid spaces (SASs) at the level of the medulla oblongata. The SAS is lined by the arachnoid externally and by the fenestrated pia internally and covers the entire brain surface. Vessels penetrating the brain are surrounded by the perivascular space. Substances, including β-glucuronidase, would gain access to the underlying parenchyma via this space (Esiri and Gay, 1990; Zhang et al., 1990). Given the dense vasculature of the brain, β-glucuronidase in the CSF would eventually penetrate most brain regions. Consistent with our work, early experiments showed that horseradish peroxidase, a tracer protein, entered the perivascular space and outlined the intraparenchymal microvasculature throughout the forebrain and brainstem after infusion into lateral ventricles (Gregory et al., 1985; Rennels et al., 1985).

β-Glucuronidase present in the extracellular spaces of the brain would be endocytosed by the cell soma (Fig. 2) and neuronal termini at that site. As shown in this work, enzyme access to underlying parenchyma profoundly reduced substrate accumulation (Fig. 4) and improved storage pathology (Figs. 5, 6) in all brain regions examined.

Reversal of established behavioral deficits

We showed that MPS VII mice were impaired in context fear conditioning. Both peripheral and CNS dysfunction can interrupt context fear conditioning. MPS VII mice have severe systemic diseases and are less active than age-matched heterozygous controls, reflected by their elevated baseline freezing before training (Fig. 7*A*). The reduced exploration in MPS VII mice may interfere with their acquisition of contextual cues in the environment and impair context fear conditioning. However, although conditioned fear response and context discrimination improved after AAV4βgluc treatment, baseline exploration activity of MPS VII mice did not, as revealed by comparable baseline freezing between treated and untreated MPS VII mice. Therefore, the impairment of context fear conditioning in MPS VII mice is probably not caused by peripheral illness but rather by CNS deficits.

Brain circuits underlying context fear conditioning involve different brain regions, including the amygdala and the hippocampus (for review, see Maren, 2001; Sanders et al., 2003). An overall improvement in context fear-conditioning assays reflects amelioration of disease in these regions. In this study, AAV4βgluc treatment improved two parameters of context fear conditioning relative to untreated MPS VII mice, the conditioned fear response, and context discrimination. After AAV4βgluc treatment, MPS VII mice had conditioned fear responses that were indistinguishable from heterozygous littermates, indicating a recovery of amygdala

function. Treated mice also showed improved hippocampal function by responding to a modified context (context 2) (Fig. 7). Together, the functional recovery of two distinct brain regions, the hippocampus and amygdala, is consistent with the global enzyme distribution (Fig. 1) and storage resolution (Fig. 5, 6) after gene transfer. Moreover, β-glucuronidase enzyme activity in deficient mice treated with AAV4βgluc was elevated significantly in the cerebellum and brainstem (Fig. 3).

In summary, we show that the existing CNS pathologies and functional deficits in an animal model of lysosomal storage disease can be reversed after a single unilateral delivery of AAV4 vectors expressing β-glucuronidase. Transduced ependyma served as a reservoir for constitutive delivery of recombinant enzyme to the CSF and for distribution throughout the brain. This modality may provide a simple, efficient manner to achieve global correction of CNS deficits inherent in many lysosomal storage diseases.

References

Abbott NJ (2004) Evidence for bulk flow of brain interstitial fluid: significance for physiology and pathology. Neurochem Int 45:545–552.

Bastedo L, Sands MS, Lambert DT, Pisa MA, Birkenmeier E, Chang PL (1994) Behavioral consequences of bone marrow transplantation in the treatment of murine mucopolysaccharidosis type VII. J Clin Invest 94:1180–1186.

Birkenmeier EH, Davisson MT, Beamer WG, Ganschow RE, Vogler CA, Gwynn B, Lyford KA, Maltais LM, Wawrzyniak CJ (1989) Murine mucopolysaccharidosis type VII. Characterization of a mouse with beta-glucuronidase deficiency. J Clin Invest 83:1258–1266.

Bosch A, Perret E, Desmaris N, Heard JM (2000) Long-term and significant correction of brain lesions in adult mucopolysaccharidosis type VII mice using recombinant AAV vectors. Mol Ther 1:63–70.

Brooks AI, Stein CS, Hughes SM, Heth J, McCray Jr PM, Sauter SL, Johnston JC, Cory-Slechta DA, Federoff HJ, Davidson BL (2002) Functional correction of established CNS deficits in an animal model of lysosomal storage disease using feline immunodeficiency virus-based vectors. Proc Natl Acad Sci USA 99:6216–6221.

Chang PL, Lambert DT, Pisa MA (1993) Behavioural abnormalities in murine model of a human lysosomal storage disease. NeuroReport 4:507–510.

Chiorini JA, Yang L, Liu Y, Safer B, Kotin RM (1997) Cloning of adeno-associated virus type 4 (AAV4) and generation of recombinant AAV4 particles. J Virol 71:6823–6833.

Davidson BL, Stein CS, Heth JA, Martins I, Kotin RM, Derksen TA, Zabner J, Ghodsi A, Chiorini JA (2000) Recombinant adeno-associated type 2, 4 and 5 vectors: transduction of variant cell types and regions in the mammalian CNS. Proc Natl Acad Sci USA 97:3428–3432.

Del Bigio MR (1995) The ependyma: a protective barrier between brain and cerebrospinal fluid. Glia 14:1–13.

Esiri MM, Gay D (1990) Immunological and neuropathological significance of the Virchow-Robin space. J Neurol Sci 100:3–8.

Frantantoni JC, Hall CW, Neufeld EF (1969) Hurler and Hunter syndromes: mutual correction of the defect in cultured fibroblasts. Science 162:570–572.

Frisella WA, O'Connor LH, Vogler CA, Roberts M, Walkley S, Levy B, Daly TM, Sands MS (2001) Intracranial injection of recombinant adeno-associated virus improves cognitive function in a murine model of mucopolysaccharidosis type VII. Mol Ther 3:351–358.

Gage FH (2000) Mammalian neural stem cells. Science 287:1433–1438.

Ghodsi A, Stein C, Derksen T, Martins I, Anderson RD, Davidson BL (1999) Systemic hyperosmolality improves β-glucuronidase distribution and pathology in murine MPS VII brain following intraventricular gene transfer. Exp Neurol 160:109–116.

Gregory TF, Rennels ML, Blaumanis OR, Fujimoto K (1985) A method for microscopic studies of cerebral angioarchitecture and vascular-parenchymal relationships, based on the demonstration of 'paravascular' fluid pathways in the mammalian central nervous system. J Neurosci Methods 14:5–14.

Griffey M, Bible E, Vogler C, Levy B, Gupta P, Cooper J, Sands MS (2004) Adeno-associated virus 2-mediated gene therapy decreases autofluorescent storage material and increases brain mass in a murine model of infantile neuronal ceroid lipofuscinosis. Neurobiol Dis 16:360–369.

Heuer GG, Passini MA, Jiang K, Parente MK, Lee VM, Trojanowski JQ, Wolfe JH (2002) Selective neurodegeneration in murine mucopolysaccharidosis VII is progressive and reversible. Ann Neurol 52:762–770.

Kornfeld S, Mellman I (1989) The biogenesis of lysosomes. Annu Rev Cell Biol 5:483–525.

Levy B, Galvin N, Vogler C, Birkenmeier EH, Sly WS (1996) Neuropathology of murine mucopolysaccharidosis type VII. Acta Neuropathol (Berl) 92:562–568.

Liu G, Martins IH, Chiorini JA, Davidson BL (2005) Adeno-associated virus type 4 (AAV4) targets ependyma and astrocytes in the subventricular zone and RMS. Gene Ther, in press.

Maren S (2001) Neurobiology of pavlovian fear conditioning. Annu Rev Neurosci 24:897–931.

Meikle PJ, Hopwood JJ, Clague AE, Carey WF (1999) Prevalence of lysosomal storage disorders. JAMA 281:249–254.

Meng XL, Shen JS, Ohashi T, Maeda H, Kim SU, Eto Y (2003) Brain transplantation of genetically engineered human neural stem cells globally corrects brain lesions in the mucopolysaccharidosis type VII mouse. J Neurosci Res 74:266–277.

Neufeld EF, Fratantoni JC (1970) Inborn errors of mucopolysaccharide metabolism. Science 169:141–146.

Neufeld EF, Muenzer J (1995) The mucopolysaccharidoses. In: The metabolic basis of inherited disease (Sriver CR, Beaudet AL, Sly WS, Valle D, eds), pp 2465–2494. New York: McGraw-Hill.

O'Connor LH, Erway LC, Vogler CA, Sly WS, Nicholes A, Grubb J, Holmberg SW, Levy B, Sands MS (1998) Enzyme replacement therapy for murine mucopolysaccharidosis type VII leads to improvements in behavior and auditory function. J Clin Invest 101:1394–1400.

Orii KO, Grubb JH, Vogler C, Levy B, Tan Y, Markova K, Davidson BL, Mao Q, Orii T, Kondo N, Sly WS (2005) Defining the pathway for Tat-mediated delivery of β-glucuronidase in cultured cells and MPS VII mice. Mol Ther 12:345–352.

Passini MA, Lee EB, Heuer GG, Wolfe JH (2002) Distribution of a lysosomal enzyme in the adult brain by axonal transport and by cells of the rostral migratory stream. J Neurosci 22:6437–6446.

Rennels ML, Gregory TF, Blaumanis OR, Fujimoto K, Grady PA (1985) Evidence for a 'paravascular' fluid circulation in the mammalian central nervous system, provided by the rapid distribution of tracer protein throughout the brain from the subarachnoid space. Brain Res 326:47–63.

Sanders MJ, Wiltgen BJ, Fanselow MS (2003) The place of the hippocampus in fear conditioning. Eur J Pharmacol 463:217–223.

Sands MS, Vogler C, Kyle JW, Grubb JH, Levy B, Galvin N, Sly WS, Birkenmeier EH (1994) Enzyme replacement therapy for murine mucopolysaccharidosis type VII. J Clin Invest 93:2324–2331.

Sly WS, Quinton BA, McAlister WH, Rimoin DL (1973) Beta glucuronidase deficiency: report of clinical, radiologic, and biochemical features of a new mucopolysaccharidosis. J Pediatr 82:249–257.

Stein CS, Kang Y, Sauter SL, Townsend K, Staber PD, Derksen TA, Martins I, Qian J, Davidson BL, McCray PBJ (2001) In vivo treatment of hemophilia A and mucopolysaccharidosis type VII using nonprimate lentiviral vectors. Mol Ther 3:850–856.

Taylor RM, Wolfe JH (1997) Decreased lysosomal storage in the adult MPS VII mouse brain in the vicinity of grafts of retroviral vector-corrected fibroblasts secreting high levels of beta-glucuronidase. Nat Med 3:771–774.

Vogler C, Birkenmeier EH, Sly WS, Levy B, Pegors C, Kyle JW, Beamer WG (1990) A murine model of mucopolysaccharidosis VII. Am J Pathol 136:207–217.

von Figura K, Hasilik A (1986) Lysosomal enzymes and their receptors. Annu Rev Biochem 55:167–193.

Xia H, Mao Q, Davidson BL (2001) The HIV tat protein transduction domain improves the biodistribution of β-glucuronidase expressed from recombinant viral vectors. Nat Biotechnol 19:640–644.

Zhang ET, Inman CB, Weller RO (1990) Interrelationships of the pia mater and the perivascular (Virchow-Robin) spaces in the human cerebrum. J Anat 170:111–123.